

## The Elasticity of Single Crystals of Lead

BY S. C. PRASAD AND W. A. WOOSTER

*Crystallographic Laboratory, Cavendish Laboratory, Cambridge, England*

(Received 3 August 1955)

Lead single crystals of some 2 cm. diameter were grown by slow cooling from the melt. Faces parallel to (100) and (110) were cut with a microtome, and polished electrolytically. The crystals obtained were perfect, at least as far as was tested by the present measurements. Spectrometer studies on the diffuse scattering at points on the lines parallel to [110],  $\bar{1}10$  and [001] passing through the reciprocal-lattice point 220 lead to the elastic ratios  $c_{12}/c_{11} = 0.78 \pm 0.05$  and  $c_{44}/c_{11} = 0.28 \pm 0.02$ . The photographic study was made on a photograph of the diffuse spot associated with the reciprocal-lattice point 400. The elastic ratios obtained were substantially the same as those given above. The known compressibility was used to obtain the absolute values as follows:

$$\begin{aligned} c_{11} &= 5.0(3), & c_{12} &= 3.9(3), & c_{44} &= 1.4(0) \times 10^{11} \text{ dyne cm.}^{-2}; \\ s_{11} &= 63.2(2), & s_{12} &= -27.7(7), & s_{44} &= 71.4(4) \times 10^{-13} \text{ cm.}^2 \text{ dyne}^{-1}. \end{aligned}$$

The main discrepancy between these values and those obtained by other methods is in the value of  $(c_{11} - c_{12})$ . The present method measures this directly and is believed to be more accurate than the previous measurements. The differences in the  $s_{ik}$ 's are a consequence of this discrepancy in  $c_{11} - c_{12}$ .

### Introduction

The ease with which single crystals of lead may be plastically deformed makes it difficult to employ static or low-frequency oscillation methods for elasticity measurement. However, two sets of observations have been made, namely by Goens & Weerts (1936), who used low-frequency torsional and flexural oscillations, and by Swift & Tyndall (1942), who used static stretching and twisting observations. The method involving diffuse X-ray reflexions avoids the possibility of plastic deformation and has been used by Lonsdale & Smith (1941, 1942) and by Lonsdale (1942). These authors were not concerned with determining the elastic constants from their diffuse photographic spots but rather with comparing the density distribution observed with that calculated on the basis of Jahn's (1942) presentation of the theory. The present work is an attempt to obtain the elastic constants from the study of diffuse X-ray reflexions using both Geiger-counter spectrometer and photographic techniques.

### Growth of crystals

The crystals of lead were grown by lowering a glass tube containing molten lead slowly through a vertical furnace. Certain features of this application of a conventional method are worth mentioning. To avoid cracking the Pyrex glass tube, it was found best to melt the lead only once and to allow it to solidify as the final crystal. The glass tube was filled with small pieces of the pure lead (Messrs Johnson, Matthey and Company—99.99% pure), evacuated and sealed; the lead was then melted in the furnace, the centre of which was at 400° C. approximately. The tube descended at a uniform rate of 5 mm. hr.<sup>-1</sup>. A hooked

capillary tube at the bottom of the tube was used to induce single-crystalline growth. After removal from the glass tube the crystal was etched in a solution consisting of hydrogen peroxide (3 parts), glacial acetic acid (2 parts), and water (1 part). Usually the whole block was a single crystal but, when it was not, the boundaries between separate crystals were readily revealed by etching for about two minutes.

### Preparation of surfaces parallel to given planes

For the spectrometer investigation the reflexion 220 and for the photographic work the reflexion 400 were used. Flat surfaces were therefore cut parallel to the (110) and (100) planes respectively. Much preliminary work was done in order to find a way of cutting and polishing such surfaces without disturbing the perfection of the crystal. In view of the softness of lead, remarkable success was achieved in the following way. Using a Unicam oscillation goniometer the cast block was orientated so that the required plane, (110) or (100), was horizontal. The trace of the horizontal plane was marked in ink round the block. The block was then cut with a hack-saw, holding the block in the hand, and using only light pressure on the saw. The surface was then cut with a standard microtome, about a millimetre thickness being removed in this way. The surface was now electrolytically polished using a solution consisting of one volume of perchloric acid (60%, specific gravity 1.58) and four volumes of acetic anhydride. The current density was 0.2 A.cm.<sup>-2</sup> and the applied voltage 50. The anode support and the cathode were of lead. Polishing was carried on for a few minutes at a time so that the temperature never rose to a dangerous point.

Polishing was carried on in this way until tests of the sharpness of the Laue reflexion showed that no further increase in perfection could be achieved. Usually about a millimetre had to be dissolved away to achieve this result. The surfaces so prepared were entirely satisfactory and showed, in particular, no mosaic spread corresponding to disordering of a surface layer. The surfaces used were about 2 cm. in diameter and inclined to the true corresponding atomic planes at not more than  $2^\circ$ . The exact orientation was in each case determined and allowed for in subsequent work.

### Spectrometer procedure and results

The following observations apply to certain directions (rekhas) passing through the reciprocal-lattice point (relp) 220. The  $K$ -values (Ramachandran & Wooster, 1951) employed are:

$$\begin{aligned} K[110]_{220} &= 2/(c_{11} + c_{12} + 2c_{44}), \\ K[\bar{1}10]_{220} &= 2/(c_{11} - c_{12}), \\ K[001]_{220} &= 1/c_{44}. \end{aligned}$$

The observations of diffuse scattering along the rekhas  $[110]$ ,  $[\bar{1}10]$  and  $[001]$  were made with two settings of the crystal, namely, in one setting the  $[001]$  axis was vertical and in the other this axis was horizontal. Corrections for divergence were applied according to the method described by Ramachandran & Wooster (1951). The second-order thermal scattering was larger in lead than in any substance previously studied. For the rekhas used in the spectrometer study the usual method of calculation was employed, although the results indicate that this method slightly over-corrects for the second-order thermal contribution to the diffuse scattering. In the photographic study described below it was necessary to calculate the second-order contribution,  $I_2$ , for a rekha having a general direction. Ramachandran & Wooster (1951) have shown that

$$I_2/I_1 = \frac{1}{2}\pi^3 k T q^2 R \cdot K'/K,$$

where  $q$  is the distance of the relp from the origin, and  $K'$  is a quantity corresponding to  $K$  which applies

to the second-order thermal scattering. It is true for several rekhas that

$$K' = K^2,$$

and even when not exactly true the difference  $K' - K^2$  is not more than 12% of the value of  $K'$ . Thus the relation

$$I_2/I_1 = \frac{1}{2}\pi^3 k T q^2 R K,$$

obtained by substituting  $K' = K^2$ , was used and a correction was made where necessary to allow for the small departure from equality of  $K'$  and  $K^2$ . Since all quantities in the equation for  $I_2/I_1$  are known, the correction to be applied on account of  $I_2$  can be found.

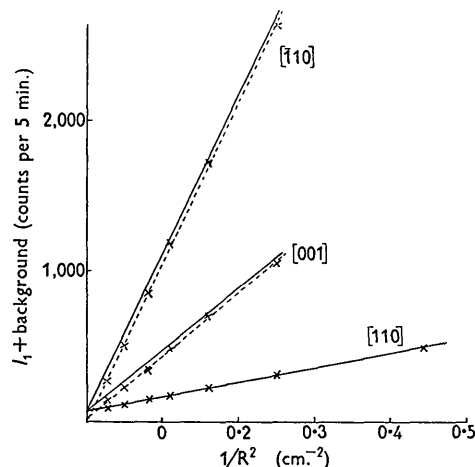


Fig. 1. Diagram showing relation between  $(I_1 + \text{background})$  and  $1/R^2$  for the spectrometer observations.

The experimental observations are given in Table 1. The distance  $R$  is measured along the rekha from the relp 220 to the point at which the diffuse intensity is measured. The radius of the Ewald sphere is taken as 50 cm. The quantities in the columns headed ' $I_1 + \text{background}$ ' are plotted against  $1/R^2$  in Fig. 1. The broken lines are the best straight lines which can be drawn through the points. The line corresponding to the rekha parallel to  $[110]$  cuts the axis of ordinates at a point corresponding to about 65 counts per 5 min. The broken lines corresponding to  $[001]$  and  $[\bar{1}10]$  cut

Table 1  
Counts in 5 min. for rekhas parallel to

$R$ (cm.)	$1/R^2$ ( $\text{cm.}^{-2}$ )	$[110]$			$[\bar{1}10]$			$[001]$		
		Total	$I_2$	$I_1 +$ background	Total	$I_2$	$I_1 +$ background	Total	$I_2$	$I_1 +$ background
1.5	0.444	495	2.9	492.1	—	—	—	—	—	—
2.0	0.250	318.7	2.2	316.5	2927	289	2638	1075	19.6	1055.4
2.5	0.160	233.4	1.8	231.6	1961	234.4	1726.6	717.8	16.0	701.8
3.0	0.111	174.6	1.4	173.2	1375.8	191.0	1184.8	499.1	12.9	486.2
3.5	0.0816	153.8	1.3	152.5	1007.3	157.6	849.7	357.8	10.4	347.4
4.5	0.0498	116.9	0.9	116.0	626.8	117.4	509.4	237.8	8.2	229.6
6.0	0.0278	100.4	0.8	99.6	348	77.0	271.0	154.6	6.3	146.3
Mean slope		985			10,540			4,110		

at points corresponding to less than this number. It is probable that the second-order correction given by the column  $I_2$  is slightly too large in the  $[001]$  and  $[\bar{1}10]$  directions.

To obtain the lines in Fig. 1 from which the evaluation of the elastic constants can be made, the full lines for  $[001]$  and  $[\bar{1}10]$  have been drawn through the point at 65 on the axis of ordinates and so as to allow a smaller and smaller departure from the dotted lines as  $1/R^2$  increases. This corresponds to the diminishing ratio of  $I_2/I_1$ . The slopes of the full lines are proportional to the corresponding  $K[ABC]_{hkl}$  values. Writing  $\chi_{12} = c_{12}/c_{11}$  and  $\chi_{44} = c_{44}/c_{11}$ , we have

$$\begin{aligned} K[110]_{220}/K[\bar{1}10]_{220} &= (1 - \chi_{12})/(1 + \chi_{12} + 2\chi_{44}), \\ K[\bar{1}10]_{220}/K[001]_{220} &= 2\chi_{44}/(1 - \chi_{12}). \end{aligned}$$

Inserting the values of the mean slope from Table 1, we have

$$\chi_{12} = 0.78(2), \quad \chi_{44} = 0.27(9).$$

The compressibility at zero pressure, derived from Bridgman's (1945) data, is  $23.3 \times 10^{-13} \text{ cm.}^2 \text{ dyne}^{-1}$ .

Using the relation

$$1/\beta = \frac{1}{3}(c_{11} + 2c_{12}) = \frac{1}{3}c_{11}(1 + 2\chi_{12}),$$

we obtain

$$c_{11} = 5.0(3), \quad c_{12} = 3.9(3), \quad c_{44} = 1.4(0) \times 10^{11} \text{ dyne cm.}^{-2}.$$

Table 1 shows the large anisotropy of the diffuse scattering, being more than ten times as large along rekha  $[\bar{1}10]$  as along the rekha  $[110]$ . This fact makes the  $\psi$ -divergence correction rise to about 10% as a maximum. This is unusually large and probably lessens to some extent the overall accuracy, which is usually  $\pm 5\%$ .

### Photographic procedure and results

A diffuse reflexion photograph (Fig. 2(a)) was taken, using a (100) face and Cu  $K\alpha$  radiation in a cylindrical

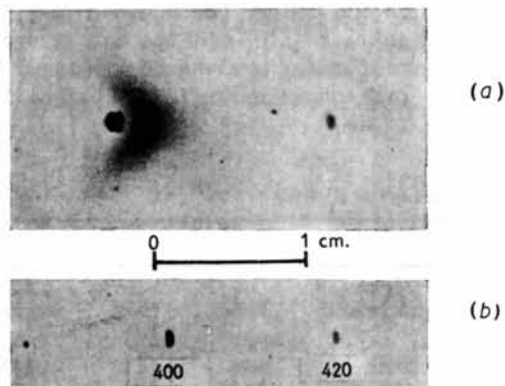


Fig. 2. (a) Diffuse reflexion photograph associated with relp 400 of lead,  $[001]$  axis vertical. On right-hand side the Bragg reflexion 420 is recorded.

(b) Oscillation photograph from same crystal face showing position of Bragg reflexion 400 relative to that of 420.

camera of radius 5.73 cm. The Bragg reflexion 400 occurs at  $\theta = 38^\circ 38'$ , and the crystal was set at an angle of incidence  $1^\circ 50'$  less than that corresponding to the Bragg angle, i.e.  $\theta - i = 1^\circ 50'$ . The Bragg setting was determined using a Geiger counter and rate meter, and the crystal was rotated on the Unicam oscillation goniometer through the required  $1^\circ 50'$  from this position. At the end of the exposure (20 hr.) the crystal was rotated so as to record the Bragg reflexion 420 on the same photograph. In Fig. 2(a) this is the reflexion on the right-hand side of the figure. A second photograph (Fig. 2(b)) was taken to record both the Bragg spots 400 and 420. By superposing Fig. 2(b) on Fig. 2(a), so that the 420 spots are on top of one another, the position of the Bragg spot relative to the diffuse spot can be determined.

The distribution of density over the diffuse spot was measured with an automatic recording microdensitometer (Wooster, 1956). The area surveyed was  $12 \times 13$  mm. and the background density was determined from the readings on the outside of this area. The 'skew correction' (Ramachandran & Wooster, 1951) was applied and the results are expressed in Fig. 3. Only

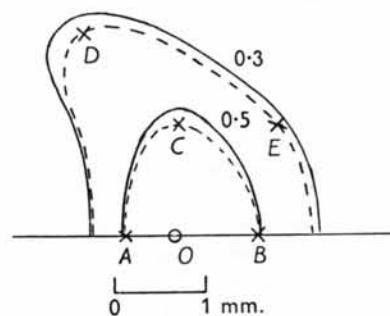


Fig. 3. Contours of density expressed as fractions of the peak density. The broken curves correspond to the contours which would be obtained if there were no divergence of the X-ray beam and if second-order scattering were absent.

half the diffuse spot is represented because there is a horizontal plane of symmetry through the spot. The full curves labelled 0.5 and 0.3 show the contours of the points at which the intensity is 0.5 and 0.3 respectively of the intensity at the centre of the spot.

### Interpretation of the diffuse spot

The point  $O$  along the centre line of the diffuse spot corresponding to the centre of circles of constant  $R$  (Hoerni & Wooster, 1952), i.e. of points at a constant distance from the relp 400, was determined from the position of the Bragg spot (Fig. 2(b)). A chart drawn for  $s = 0.031$ , corresponding to  $\theta - i = 1^\circ 50'$ , was superimposed on the microdensitometer record so as to read off the  $\bar{\rho}$ ,  $\bar{\varphi}$  angles of any point on it. The  $R$ -chart was also used to determine the distance of any point from the relp 400.

The observed intensities are due to first-order and

second-order thermal scattering, and, although it is possible for most crystals to neglect the second-order scattering, it is necessary to take it into account with lead. This was done in the following way. A  $K$ -surface giving the values of  $K[ABC]_{100}$  in all directions was calculated, using the values of the  $\chi_{12}$  and  $\chi_{44}$  already determined by the spectrometer investigation. (Approximate values of these constants could have been obtained from the photograph alone.) The  $K$ -surface was plotted with an orientation corresponding to that of the photograph and, using the  $R$ -circles, the theoretical intensity distribution for first-order scattering alone was determined. The second-order thermal scattering was now calculated in the manner described in the previous paragraph and the values of  $I_1+I_2$  were plotted as before round the calculated 0.5 contour. A second correction was made to allow for the divergence of the X-ray beam. The size of the Bragg spot, when of the same density as the diffuse spot, was about  $1 \times \frac{1}{3}$  mm. The microdensitometer diagram was plotted on a scale of 24 mm. = 1 mm. on the film. Therefore, a rectangle  $24 \times 8$  mm. was drawn on tracing paper and divided into three squares  $8 \times 8$  mm. This was superposed on the plot of the calculated ( $I_1+I_2$ ) values and the values at the centre of each square were noted. The mean of the three values was taken as the averaged value over the whole spot. The procedure was applied in the region near to each contour and the displacement due to the divergence was determined. The sum of the displacements due to the second-order thermal scattering and the divergence were added. The uncorrected  $I_1$  curve and the ( $I_1+I_2$ ) curve corrected for divergence were calculated for particular values of  $\chi_{12}$  and  $\chi_{44}$ . The difference between them is assumed to be the same as the difference between the  $I_1$  experimental curve and that actually observed and given in Fig. 3. The broken curves in Fig. 3 show the position of the contours for  $I_1$  after correcting for second-order thermal scattering and for divergence. In principle any three points on the contoured diagram of Fig. 3 can yield values of the elastic ratios  $\chi_{12}$ ,  $\chi_{44}$ . For each point the angular coordinates  $\bar{\rho}$ ,  $\bar{\varphi}$  are read off and, bearing in mind the orientation of the crystallographic axes relative to the diagram ( $x$ ,  $90^\circ$ ,  $51^\circ L$ ;  $y$ ,  $90^\circ$ ,  $39^\circ R$ ;  $z$ ,  $0^\circ$ ,  $0^\circ$ ), the direction cosines ( $u, v, w$ ) of the rekha can be calculated. Also, the value of  $R$  is read off from a chart and hence the quantity  $(R_0/R)^2$  is determined. The values for the points  $ABCDE$  of Fig. 3 are given in Table 2.

If  $I$  is the intensity at a point on the photograph,

Table 2

Point	$\bar{\rho}$ ( $^\circ$ )	$\bar{\varphi}$ ( $^\circ$ )	$I$	$(R_0/R)^2$	$K_{\text{obs.}}$
<i>A</i>	90	17 <i>L</i>	0.5	0.9	0.56
<i>B</i>	90	28 <i>R</i>	0.5	0.76	0.66
<i>C</i>	57	1 <i>R</i>	0.5	0.66	0.76
<i>D</i>	43	28 <i>L</i>	0.3	0.33	0.91
<i>E</i>	60	32 <i>R</i>	0.3	0.51	0.59

corresponding to the first-order thermal scattering from an infinitely narrow and parallel beam, then the experimental value of  $K$  is given by  $K_{\text{obs.}} = I/(R_0/R)^2$ .

For each of the points  $A-E$  in turn, the value of  $K$  is now calculated for a range of values of  $\chi_{12}$  and  $\chi_{44}$  and the appropriate ( $u, v, w$ ) values. For two points, e.g.  $A$  and  $B$ , the ratio of the calculated  $K$ -values is plotted on a diagram in which the co-ordinate axes are  $\chi_{12}$  and  $\chi_{44}$ . Over small ranges of  $\chi_{12}$  and  $\chi_{44}$  the lines of constant value for  $K_A/K_B$  (calculated) are straight. Thus on this diagram a single straight line can be drawn corresponding to the observed  $K_A/K_B$  ratio. In the same way lines for  $K_A/K_C$ ,  $K_C/K_A$  and  $K_D/K_E$  are drawn. Ideally these lines would intersect nearly perpendicularly and all pass through the point corresponding to the true values of  $\chi_{12}$ ,  $\chi_{44}$ . In this instance, however, the lines are inclined at a small angle to one another and do not intersect. This is due to the restricted range of ( $u, v, w$ ) values. However, the mean line passes through the points corresponding to the combinations of values

$$\chi_{12} = 0.76, \chi_{44} = 0.30; \quad \chi_{12} = 0.78, \chi_{44} = 0.28;$$

$$\chi_{12} = 0.84, \chi_{44} = 0.21.$$

More photographs would be necessary to determine the ratios more precisely. Thus, within the accuracy of the measurement, the result obtained by the photographic method, using the relp 400, agrees with the spectrometer observations on the relp 220.

## Discussion

Previous determinations of the elastic constants of lead are compared with the present work in Table 3.

Table 3. *Elastic constants of lead*

(Values of  $c$  are given in units of  $10^{11}$  dyne cm. $^{-2}$ ; values of  $s$  in units of  $10^{-13}$  cm. $^2$  dyne $^{-1}$ )

	Goens & Weerts (1936)	Swift & Tyndall (1942)	Present work
$c_{11}$	4.77	4.66	5.0(3)
$c_{12}$	4.03	3.92	3.9(3)
$c_{44}$	1.44	1.44	1.4(0)
$c_{11}-c_{12}$	0.74	0.74	1.10
$\chi_{12}$	0.845	0.841	0.78(2)
$\chi_{44}$	0.302	0.309	0.27(9)
$s_{11}$	92.7	92.8	63.(2)
$s_{12}$	-42.5	-42.4	-27.(7)
$s_{44}$	69.4	69.4	71.(4)
$s_{11}-s_{12}$	135.2	135.2	90.9

The values of Goens & Weerts refer to adiabatic conditions whereas the static method of Swift & Tyndall leads to isothermal values. The difference on this account is small and does not affect the discrepancy relating to ( $c_{11}-c_{12}$ ) and the  $s_{ik}$ 's. The present value of ( $c_{11}-c_{12}$ ) is 1.10 and higher than the previous

values by more than can be explained by the experimental error of the present measurements. In the previous work the value of  $(c_{11}-c_{12})$  did not occur alone, as in the expression for  $K[\bar{1}10]_{220}=2/(c_{11}-c_{12})$ , but was involved in a more complex way with the elastic constants. The value of  $K[\bar{1}10]_{220}$  is sensitive to a change in  $(c_{11}-c_{12})$ , and the slope of the corresponding line in Fig. 1 would have to be changed by an amount far outside the experimental error in order to bring the result into conformity with the value 0.74. One factor must not be overlooked and that is the possible failure of the diffuse reflexion theory owing to the large amplitude of thermal vibration of the lead atoms. However, the straight lines of Fig. 1 suggest that there is no breakdown of the theory as far as it applies to the first-order thermal scattering. Further, the photographic determination was carried out on points having no special relation to the rekha direction  $[\bar{1}10]$  and the results are consistent with those obtained by the spectrometer study.

One of the authors (S. C. P.) feels a great pleasure in recording his gratitude to the Government of Bihar, India, for the grant of a research scholarship and the leave for the period in which this work has been carried out.

#### References

- BRIDGMAN, P. W. (1945). *Proc. Amer. Acad. Arts Sci.* **76**, 9.  
 GOENS, E. with WEERTS, J. (1936). *Phys. Z.* **37**, 321.  
 HOERNI, J. A. & WOOSTER, W. A. (1952). *Acta Cryst.* **5**, 626.  
 JAHN, H. A. (1942). *Proc. Roy. Soc. A*, **179**, 320.  
 LONSDALE, K. (1942). *Proc. Phys. Soc.* **54**, 314.  
 LONSDALE, K. & SMITH, H. (1941). *Nature, Lond.* **148**, 628.  
 LONSDALE, K. & SMITH, H. (1942). *Nature, Lond.* **149**, 21.  
 RAMACHANDRAN, G. N. & WOOSTER, W. A. (1951). *Acta Cryst.* **4**, 335, 431.  
 SWIFT, I. H. & TYNDALL, E. P. T. (1942). *Phys. Rev.* **61**, 359.  
 WOOSTER, W. A. (1956). In the Press.

*Acta Cryst.* (1956). **9**, 42

## An Apparent Anisotropic Debye-Waller Factor in Cubic Crystals

BY R. J. WEISS, J. J. DEMARCO AND G. WEREMCHUK

*Ordnance Materials Research Office, Watertown Arsenal, Watertown, Mass., U.S.A.*

AND L. CORLISS AND J. HASTINGS

*Brookhaven National Laboratories, Upton, New York, U.S.A.*

(Received 14 July 1954)

Neutron and X-ray diffraction studies on  $\alpha$  brass (70–30 f.c.c.) have revealed that the integrated intensities are reduced by a Debye-Waller temperature factor  $\exp(-2B(\sin\theta/\lambda)^2)$ , where  $B$  is not only a function of the characteristic temperature  $\theta$  and the absolute temperature  $T$ , but also a function of crystal direction, contrary to present theories for cubic crystals. The effect is very marked in comparing the 222 and 400 peaks both as to their relative intensities and their change in intensity with temperature from liquid nitrogen to room temperatures.

In the course of neutron diffraction studies of cold-worked brass (f.c.c.) (Weiss, Clark, Corliss & Hastings, 1952) it was found that the relative intensities of the 200 to the 111 peaks in cold-worked as well as annealed brass was 6% smaller than calculated. The intensities of neutron powder diffraction peaks in transmission for a f.c.c. lattice are given by

$$I \propto J_{hkl} \exp[-\mu h \sec \theta] \exp[-2B(\sin \theta/\lambda)^2/\sin^2 2\theta],$$

where  $J_{hkl}$  is the multiplicity,  $\exp[-\mu h \sec \theta]$  is the absorption factor and  $\exp[-2B(\sin \theta/\lambda)^2]$  is the Debye-Waller temperature factor. Except for the Debye-Waller factor, all factors in the intensity expression are accurately defined. Extinction effects are negligible in neutron diffraction powder patterns for the 1 Å neutrons used in these measurements. The

volume of the sample irradiated was approximately 60 cm.<sup>3</sup> of 325 mesh powder, which makes preferred orientation effects negligible. The absorption factor is directly determined by transmission of the incident beam. The ratio of the absorption factor between the 111 peak,  $2\theta = 30.4^\circ$  and the 200 peak  $2\theta = 35.2^\circ$  is considered accurate to 0.1%. After applying a characteristic temperature of 310° K. (expected from elastic constants) in the Debye-Waller factor the ratio of the 200 to the 111 peaks was too low by  $6 \pm \frac{1}{2}\%$ . By artificially invoking a characteristic temperature of 215° K. to the 200 peak (the 111 peak remaining 310° K.) agreement was obtained. Neutron measurements on copper and nickel revealed the effect to be only about  $2 \pm \frac{1}{2}\%$ .

The measurements were continued with X-rays